

Decorating the Edges of a 2D Polymer with a Fluorescence Label

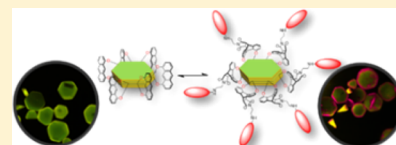
Yingjie Zhao,[†] Richard H. M. Bernitzky,[†] Max J. Kory,[†] Gregor Hofer,[†] Johan Hofkens,[‡] and A. Dieter Schlüter^{*,†}

[†]Institute of Polymers, Department of Materials, Swiss Federal Institute of Technology, ETH Zürich, Vladimir Prelog-Weg 5, 8093 Zürich, Switzerland

[‡]Division of Molecular Imaging and Photonics, Department of Chemistry, KU Leuven, Celestijnenlaan 200 F, 3001 Heverlee, Belgium

S Supporting Information

ABSTRACT: This work proves the existence and chemical addressability of defined edge groups of a 2D polymer. Pseudo-hexagonally prismatic single crystals consisting of layered stacks of a 2D polymer are used. They should expose anthracene-based edge groups at the six (100) but not at the two pseudo-hexagonal (001) and (00 $\bar{1}$) faces. The crystals are reacted with the isotopically enriched dienophiles maleic anhydride and a C18-alkyl chain-modified maleimide. In both cases the corresponding Diels–Alder adducts between these reagents and the edge groups are formed as confirmed by solid state NMR spectroscopy. The same applies to a maleimide derivative carrying a BODIPY dye which was chosen for its fluorescence to be out of the range of the self-fluorescence of the 2D polymer crystals stemming from contained template molecules. If the crystals are excited at $\lambda = 633$ nm, their (100) faces and thus their rims fluoresce brightly, while the pseudo-hexagonal faces remain silent. This is visible when the crystals lie on a pseudo-hexagonal face. Lambda-mode laser scanning microscopy confirms this fluorescence to originate from the BODIPY dye. Micromechanical exfoliation of the dye-modified crystals results in thinner sheet packages which still exhibit BODIPY fluorescence right at the rim of these packages. This work establishes the chemical nature of the edge groups of a 2D polymer and is also the first implementation of an edge group modification similar to end group modifications of linear polymers.



INTRODUCTION

Two-dimensional (2D) polymers and other 2D materials currently attract considerable attention because they exhibit properties that—in reflecting their dimensionality—are different from common three-dimensional materials.^{1,2} One way to synthesize 2D polymers rests upon the so-called single crystal approach.³ In this approach trifunctional monomers are pre-organized in layered crystals such that the reactive groups of neighboring monomers, typically anthracenes, form tight pairs [face-to-face (*ftf*) stacking]. A photochemical stimulus then brings about the reaction between them. As irradiation continues, eventually all pairs are converted into the covalent cross-links of the two-dimensional networks that form in each layer of the crystal.³ The final crystal is then composed of an array of a huge number of 2D polymer sheets placed on top of one another for example in the crystallographic *c* direction. Ideally this geometrically confined polymerization proceeds in a topochemical fashion.⁴ This means that the internal changes associated with the reaction do not prevent a single crystal to be converted into another single crystal. In such a case, structure analysis of the resulting 2D polymer is particularly easy because XRD can be applied.^{3c,d}

The term “2D polymer” is currently under discussion, but it seems that an increasing number of laboratories accept the definition which was put forward a couple of years back and refined recently.^{1,2} According to it, 2D polymers are monolayer covalent sheets with a tiled structure. The tiles are the topologically planar repeat units (RUs). At the edges of a sheet are end groups, which—to differentiate from the well-known

end groups of linear polymers—we refer to as edge groups. We recently reported the rotor-shaped, anthracene-based monomer **1** and the hexaprismatic 2D polymer crystals obtained from it by photochemically triggered dimerization ($\lambda = 465$ nm) of *ftf*-stacked anthracene units of neighboring monomers in the monomer crystals (Figure 1a).^{3d} The monomers are held in place by the same compound **1**, which also acts as template (monomer:template = 2:1), and by solvent molecules. The polymerization can be pushed to full conversion, whereby all internal functional groups of the monomers (but not those of the template molecules) are converted into cross-links, while the groups that happen to reside at the edge of the monomer crystal should remain unchanged, caused by the lack of coupling partner (Figure 1a, blue circles). For these crystals we use the abbreviation C. The presentation of anthracene edge groups at some crystal surfaces in principle offers the opportunity to prove their presence by selective modification before or after exfoliation of the 2D polymer single crystal into sheet packages and single sheets.

End groups of linear polymers play a fundamentally important role. Not only are they of importance for molar mass determination and the prevention of unzipping reactions but also they may provide surface adhesion, compatibility in blends, and solubility. Furthermore, they are the key units for the synthesis of block copolymers. Thus, it is of great interest not only to create 2D polymers but also to explore whether

Received: May 27, 2016

Published: June 27, 2016

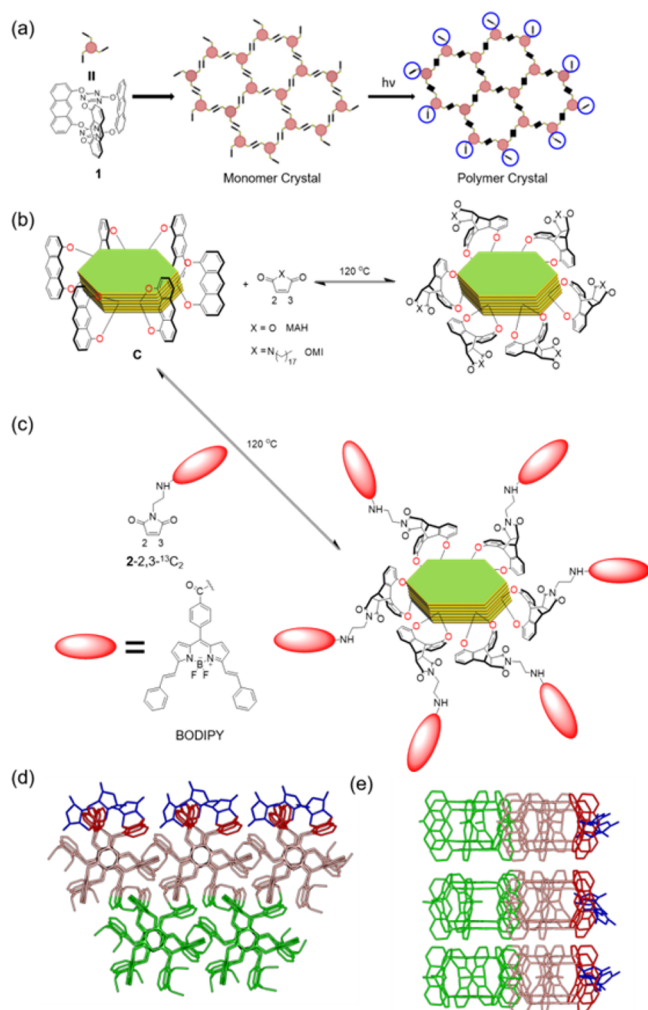


Figure 1. (a) Single-crystal approach employed for synthesis of 2D polymer. Note that the voids between the monomers are filled with template and solvent molecules which are omitted here for clarity. A third of the monomer molecules serve as unreactive templates. (b) Synthetic scheme for surface functionalization of the 2D polymer crystal through Diels–Alder reaction. Note that the anthracene units shown refer to one of the many sheets of which the crystal is composed. The individual layers of the crystals are slightly shifted relative to one another, which is meant to emphasize the stacking of sheets but has no crystallographic significance. (c) Synthetic scheme for surface modification of the 2D polymer crystal at its six (100) faces by using a maleimide reagent with BODIPY dye. (d,e) Schematic of the MAH modified 2D polymer crystal from the top (d) and from the side (e). Color code: green, bulk RU or template; light red, outermost RU or template at the crystal (100) face the initially active edge anthracene unit of which (dark red) has reacted with MAH (blue).

these sheet-like entities carry the proposed edge groups and to show that these edge groups can in fact be chemically modified in a pre-determined fashion. While this will widen the impact of 2D polymers as it happened for linear polymers, it will also provide an opportunity to influence the exfoliation process, which sometimes can be challenging. However, given the extremely high molar masses expected for 2D polymers (estimated in the range of billions of Da), the ratio between edge groups and repeat units will be very low and analytics are likely to turn complicated. If a goal such as edge modification is to be pursued, for handling reasons it seemed easier to work with sheet crystals rather than single sheets or sheet packages.

However, aside from the concentration issue there is also the additional complication that the exact molecular-scale structure at the crystal faces is not normally known. Even the highest quality XRD data do not provide information on holes, protrusions, terraces, and caves. One cannot, therefore, expect to obtain conversion numbers when chemically addressing sheet edges.

Chemical modifications of crystalline materials are not uncommon. They have been routinely performed to modify faces, channels and pore walls of zeolites⁶ and of metal–organic frameworks (MOFs),⁷ for example. For such purposes fluorescence dyes have also been used.⁸ Crystals of synthetic^{9,10} and natural polymers^{11,12} have been modified at their surface both in face-selective and unselective fashion. Modifications of the surfaces of organic crystals, however, have practically not been reported, as there are no reported attempts to modify 2D polymers at their edges. The work by Ciscek et al. is a noticeable exception regarding the former, who modified tetracene and rubrene single crystal surfaces by using Diels–Alder (DA) chemistry with a collection of dienophiles including maleic acid anhydride (MAH) and *N*-methyl maleimide.¹³ Another interesting example regards a COF microcrystal the surface of which was decorated with a fluorescence tag.¹⁴ For comprehensiveness, we note that the main planes of nanosized covalent sheets described by Kim et al. have been decorated via host–guest interactions and covalent bonds.¹⁵ In the present context it is also worth noting that edge modifications of monodisperse nanographenes have recently been published.¹⁶ They, however, involve comparably small entities (few nm range) and have been carried out in solution. Finally, we note that whenever surfaces are involved in chemical reactions the issue of unspecific physisorption versus chemical reaction arises. The experiments performed have therefore to be selected such that they can differentiate these possibilities and unequivocally prove that chemical reaction has taken place.

We here report the chemical modification of the fully polymerized crystals C with two different average sizes (1–2 μm , C_{small} , and 10–20 μm , C_{large}) with the powerful dienophiles maleic anhydride (MAH) and *N*-octadecylmaleimide (OMI) (Figure 1b). The crystals are pseudohexagonally shaped with the crystallographic *c*-direction perpendicular to the hexagonal faces. 2D polymer sheets are arranged perpendicular to the *c*-axis and thus the edge groups are exposed at the six (100) crystal faces. The different sizes of C were chosen because they have different volume to surface ratios which allows cross-checking analytical results obtained on the crystals by whether or not they reflect this ratio. For the modifications fully polymerized crystals were used and they were first carried out with MAH and OMI to prove the feasibility of the anticipated chemical reaction. To tackle the sensitivity issue, both components were used in ¹³C-isotopically labeled form (at C-2 and C-3) (Figure 1b) which should result in a signal enhancement of a factor of 10 000. In this context it is worth noting that the ratio between edge groups and internal RUs is 1:5000 for C_{large} (calcd for 20 μm) and 1:600 for C_{small} (calcd for 2 μm). The NMR signals for the decorated C_{small} are therefore expected to rise considerably beyond the regular signals while for C_{large} they should appear almost as normal.

RESULTS AND DISCUSSION

The crystals obtained after modification were analyzed by ¹³C CP/MAS NMR spectroscopy to confirm the bond formation as required for the proposed DA reaction. After this initial proof

of reactivity, we concentrated on attaching a fluorescence label instead of simple dienophiles (Figure 1c). This was attempted by the same DA chemistry for which purpose the near-infrared *N*-substituted maleimide boron dipyrromethene (BODIPY) dye, **2**, was synthesized (Scheme S1). This dye was chosen because it emits at $\lambda = 660$ nm which is out of the fluorescence range of C tailing up to $\lambda = 640$ nm. This long wavelength emission of C is not caused by the 2D polymer within C but rather by the unconsumed template molecules which fill the voids of the 2D polymer inside the crystal.

The dye-modified crystals were investigated by confocal laser scanning microscopy (CLSM) equipped for recording lambda scans. A lambda scan records a series of individual images, each image at a specific wavelength, within a wavelength range defined by the user. When applied to a particular point in the image, the emission spectrum at that position can be recorded if one scans in small enough steps. Here measuring in the lambda mode would allow confirming the expected exclusive edge modification at the (100) faces by rim-selective fluorescence emission. In order to differentiate unspecific adsorption and covalent connection of the BODIPY-containing maleimide reagent, this reagent was also synthesized and used with ^{13}C -isotopically enriched C-2 and C-3 position. The formation of the expected DA adduct was confirmed by solid-state NMR spectroscopy (Figure 2g,h). While decreasing in its intensity, the rim fluorescence remained visible, even for thin sheet packages obtained from micromechanical exfoliation.

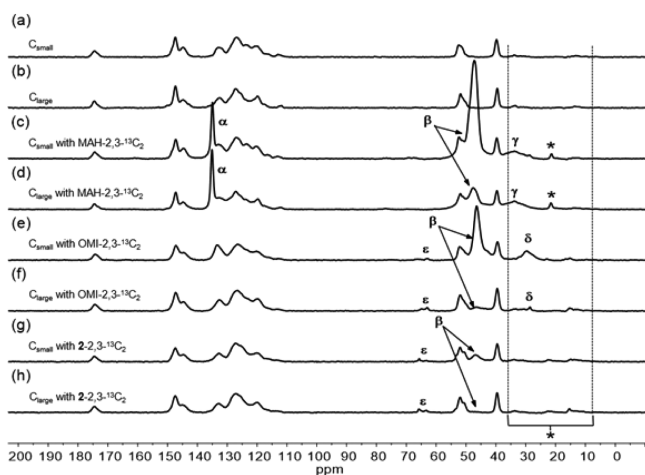


Figure 2. ^{13}C CP/MAS spectra of (a) C_{small} ; (b) C_{large} ; (c) C_{small} after reaction with MAH-2,3- $^{13}\text{C}_2$; (d) C_{large} after reaction with MAH-2,3- $^{13}\text{C}_2$; (e) C_{small} after reaction with OMI-2,3- $^{13}\text{C}_2$; (f) C_{large} after reaction with OMI-2,3- $^{13}\text{C}_2$; (g) C_{small} after reaction with 2-2,3- $^{13}\text{C}_2$; and (h) C_{large} after reaction with 2-2,3- $^{13}\text{C}_2$.

The synthesis of the monomer, its crystallization, and its polymerization ($\lambda = 465$ nm, 3 h) have been reported.^{3d,5} The C_{large} crystals were obtained following the published protocol, while C_{small} were obtained from monomer crystals the size of which was kept small by pouring a hot 2-cyanopyridine solution of the monomer directly into methanol. The polymerization conversions were proven to be quantitative by XRD among other methods. While the shape of the large crystals was uniformly pseudohexagonal, the small crystals were less regular because of the abrupt quenching process.

As mentioned above, the precise molecular structure of the outermost layer of crystals which form the crystal faces is not

normally known. High-resolution AFM imaging can in principle shed some light onto this. Since one of the intentions of the present work was to attach a bulky fluorescence dye to 2D polymer sheet edges that form a crystal face, we were interested to at least qualitatively assessing the accessibility of the (anthracene) edge groups in C. We therefore constructed a molecular model of a reactive (100) face of C from XRD data, two perspectives of which are shown in Figures 1d,e with the anthracenes having reacted with parent MAH (for simplicity). This concerns all anthracenes irrespective of whether they are edge groups of the 2D polymer or rather belong to the not covalently bound template. As can be seen from the representation of three consecutive sheets, there is not much steric crowding around the DA adducts which made us optimistic regarding the key reaction, which was the attachment of the dye. Note that this model is idealized and it may well be that the faces contain holes and caves and it is by no means clear that on a real crystal all edge groups can in fact be reached by a reagent. In particular it is unknown whether the template molecules right at the edge are actually present or “fall out” of the crystal leaving empty niches behind. For graphical representations of the (100) [and (001)] surfaces of the crystals without template molecules, see Figure S1. Because of the absence of through-pores only the outermost template molecules can fall out. The remaining large majority of templates can only leave the crystal during exfoliation.

The first modification reactions were performed with MAH. Initially, 50 mg amounts of C_{small} and C_{large} crystals and 500 mg of MAH were put into a sealed tube under argon and heated to 120 °C for 12 h. Working in neat reagent ensures maximum concentration of the dienophile in this heterogeneous reaction. Thereafter the crystals were washed five times each with CH_2Cl_2 , diethyl ether, and methanol and then dried under vacuum. The crystals were examined by optical microscopy before and after the process and found to remain unchanged (Figures S2 and S3). Thus, neither did the MAH serve as exfoliation agent nor did the conditions lead to any destruction of the crystals. To prove the reaction between MAH and edge anthracenes the crystals were investigated by IR spectroscopy. However, even for C_{small} not only was the signal due to the anhydride moiety of MAH very weak (Figure S4) but also it could not be differentiated whether it was due to covalently bonded MAH. MAH could alternatively have been physisorbed to the crystal surface or taken up into the crystal. Similar results were obtained with TGA-MS and pyrolysis-GC/MS (Figures S5–S7). Extensive washings did not have an impact.

To clarify this important issue unequivocally, we resorted to ^{13}C CP/MAS NMR spectroscopy using isotopically labeled MAH and now also OMI reagents (labeled at C-2 and C-3). Reactions and workup were performed as in the case of unlabeled MAH. Figure 2 shows the results. For comparison, Figure 2a,b contains the solid-state NMR spectra of the parent crystals C_{small} and C_{large} . Figure 2c,d shows the spectra of the reaction products with labeled MAH. Two signals at $\delta = 135$ ppm (α) and $\delta = 47$ ppm (β) are immediately apparent. Interestingly for both the large and the small crystals the low field signal α appears in a constant intensity ratio to all other signals, while the intensity of the high field signal β strongly depends on crystal size. This suggests that α is due to MAH somehow taken up into the crystal, while β is due to the expected MAH DA adduct. This latter assignment was confirmed by model studies (for details, see Supporting Information, section S1e) and is in line with reported shifts

of such DA adducts.¹⁷ Why and how MAH is taken up into the crystals is not yet understood.

Besides these two signals there also appeared a broad low intense signal at $\delta = 35$ ppm (γ) which has not yet been assigned. Figures 1e,f present the outcome with labeled OMI. In contrast to MAH there is neither an indication for incorporation into the crystal nor for unspecific physisorption, while there is again a clear signature for the anticipated DA reaction due to a signal at $\delta = 46$ ppm which is again referred to as β . The high field signal at $\delta = 29$ ppm (δ) is caused by the C₁₈ alkyl chain. The small peak at $\delta = 65$ ppm (ϵ) has not been assigned. The signals from 35 to 5 ppm and at $\delta = 22$ ppm in Figure 2c,d are due to the spinning side bands and are marked (*).

There are three main conclusions to be drawn from these spectra. First, there is clear evidence for edge anthracene units to be able to react with both dienophiles MAH and OMI in the expected DA fashion. The signals of the corresponding DA adducts at $\delta = 47$ ppm and $\delta = 46$ ppm are in fact observed. Second, the different sizes in starting crystals are reflected in the signal intensities of the products. Thus, for both MAH and OMI the intensities of their DA adduct signals are much larger for the small crystals than for the large ones. Third, the signal intensities of the OMI adducts to edge anthracenes are lower than for the corresponding MAH adducts for both crystal sizes. While this is not in agreement to the observed reactivity differences between MAH and parent maleimides,¹⁸ it may well reflect the fact that OMI carries a large substituent, the C₁₈ chain. This may not only reduce the reactivity of this dienophile in general but also in regard to accessing edge anthracenes "hidden" in niches. If this interpretation holds true it would point toward conversion limitations associated with reagent size, but it is clearly too early to expand on this aspect. The reason why seemingly only MAH is taken up into the crystals may have something to do with its small size.

Next we turned our attention to the edge-selective modification of 2D polymers with a fluorophore. On the basis of the findings presented above, the near-infrared fluorescent dye **2**, based on BODIPY carrying a maleimide linking unit, was synthesized (Scheme S1) and reacted with the crystals C_{large} (Figure 1c). The reaction conditions were similar except for using the dye in toluene solution (60 mM) rather than neat. The initial fluorescence studies were carried out using the dye-modified crystals as obtained, followed by studies using micromechanically cleaved material. Two aspects were first looked into. Do crystals that happen to lie on the substrate with their hexagonal faces fluoresce at the rims only and does the wavelength of the emission allow an unequivocal assignment to the dye rather than a template?

Figure 3 shows typical images obtained using a CLSM with an option for the lambda mode. The images in Figure 3a–c refer to unmodified crystals. At an excitation wavelength of $\lambda = 488$ nm, all crystals emit light at all faces (Figure 3a). At an excitation wavelength of $\lambda = 633$ nm, there is no visible emission, which is a clear indication that the template fluorophores are not excited at this wavelength (Figure 3b). Figure 3c represents the same section in transmission mode. In Figure 3a,c, a crystal is highlighted by a white circle that fell over and does not present its pseudo-hexagonal face therefore but rather the (100) faces with all the edge groups. Comparing the image in transmission mode (Figure 3c) of this crystal with the fluorescence mode (Figure 3a), the features do not have the

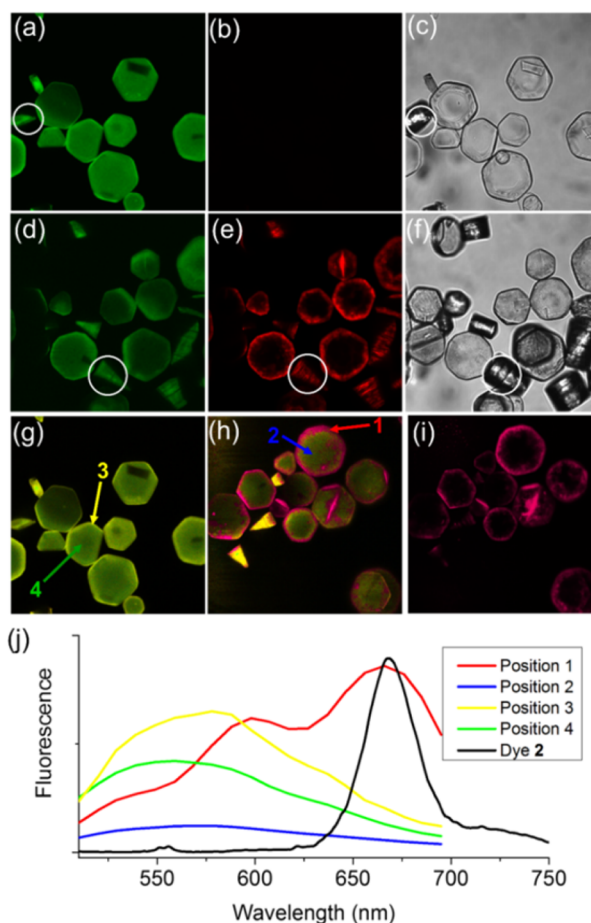


Figure 3. CLSM images of unmodified crystals excited at (a) 488 and (b) 633 nm. (c) Transmission image of unmodified crystal. CLSM images of modified crystals excited at (d) 488 and (e) 633 nm. (f) Transmission image of modified crystal. (g) Lambda scanning images (resolution: 9 nm) of unmodified crystals excited at 488 nm, and of BODIPY dye 2-modified crystals excited at (h) 488 and (i) 633 nm. (j) Uncorrected fluorescence spectra taken at the positions 1–4 marked in (g) and (h) under CLSM conditions and of the BODIPY dye 2 in CH₂Cl₂ (excited at 488 nm).

same shape. This is a consequence of working at the focal plane of flat laying crystals.

The images in Figure 3d–f refer to BODIPY-modified crystals. When excited at $\lambda = 488$ nm, again the crystals emit from all faces (Figure 3d). When excited at $\lambda = 633$ nm, however, the horizontally lying crystals emit from their rims only (Figure 3e). Overview images are available in Figure S8. Figure 3f shows the same section in transmission mode. While Figure 3e points in the desired direction, it was nevertheless necessary to confirm that the emission spectrum truly belongs to the dye. We therefore applied the lambda mode of the CLSM for unmodified crystals (Figure 3g) and modified crystals at two different excitation wavelengths, $\lambda = 488$ and 633 nm (Figure 3h,i). While the excitation at 488 nm already shows strong emission from the rim together with bulk emission from the crystal, excitation at 633 nm clearly makes only the rims to appear. Figure 3j finally shows the fluorescence spectra taken at the positions indicated 1–4 in Figure 3g,h together with the solution spectrum of the dye molecule **2** in CH₂Cl₂. The spectra taken at position 1 and taken of the dye in solution show virtually the same maximum emission wavelength with

the former showing broader signals owing to the limited resolution of the lambda mode recording.

In a control experiment to check whether there is non-specific adsorption of the dye-containing reagent, the unmodified crystals were stirred in toluene with the reagent under conditions (25 °C) where the DA reaction takes place either very slowly or not at all. Interestingly, fluorescence analysis also showed bright rims albeit in much lower intensity. It was thus necessary in this case to also unequivocally confirm the covalent connection that the above experiments had suggested. For this purpose the ^{13}C -isotopically labeled form of the BODIPY dye reagent 2-2,3- $^{13}\text{C}_2$ was synthesized (Scheme S1) and reacted with the crystals under the same conditions as had been applied for non-isotopically enriched dye-reagent (120 °C in toluene in a sealed tube). The ^{13}C CP/MAS spectra of C_{small} shows a signal at $\delta = 46$ ppm which clearly corresponds to the DA adduct (Figure 2g). As expected, the intensity of this signal for C_{large} is much lower than for C_{small} (Figure 2h) which renders it virtually invisible. This finally proves that the surface of 2D polymer crystal can be covalently modified by the BODIPY dye at the expected edge positions. The reason for the preferred physisorption at the (100) rather than the pseudo-hexagonal faces is not known at present. It is interesting to note in this context that the geometry of the holes left behind by “fallen out” template molecules differs between the faces. While for the (100) faces the holes are rather niches or caves, for the hexagonal faces they are more like a well (Figure S1).

In the next step, the large dye-decorated crystals $C_{\text{large,dye}}$ were subjected to micromechanical exfoliation using Nitto tape (SPV 224P). The crystals were sprinkled onto this adhesive tape, which was then folded onto itself and peeled apart about 50 times. Subsequent sheet package transfer onto microscopy coverslips was performed by firmly pressing the Nitto tape onto a conventional transparent adhesive tape which then was turned upside down and placed on the cover slid. This sample was then directly used for CLSM investigations. As for the crystals, BODIPY fluorescence was observed at the package rims though with reduced intensity (Figure S9). The thickness of the packages is difficult to determine in this setup. Preliminary estimates by AFM of the thinnest features in Figure S9 suggest a range of a few 10s nm.

CONCLUSION

In summary, the dienophiles MAH and OMI can be covalently connected to edge anthracene units presented at the six (100) faces of the 2D polymer single crystals obtained through photochemically triggered polymerization of single crystals of monomer 1. The connection proceeds through conventional DA reaction. This statement is largely based on solid state NMR spectroscopy using isotopically labeled MAH and OMI reagents. The same chemistry was further employed to attach a fluorescence dye to the same faces and thus to the sheet edges. Accordingly, the crystal rims rather than the bulk of these crystals emit in the range of the dye used. This finding has important consequences. First, it proves the proposed chemistry (anthracenes) at the edges of the 2D polymer used for modification. Neither XRD nor analytical techniques such as IR, UV/vis, and fluorescence spectroscopy or solid-state NMR spectroscopy allow for identification of unaltered edge groups because of their extremely low concentration. Second, it proves that a significant fraction of the edge anthracenes is actually accessible even to spatially demanding reagents,

although conversions in the classical sense cannot be given. For this, more detailed insights into the exact molecular structure of crystals at all their faces would be required including knowledge about the fate of the topmost template molecules.

An example may illustrate what we believe should now be possible: The 2D polymer used in the present study undergoes depolymerization at about 180 °C. Supposed single sheets or thin sheet packages of this polymer are treated with a focused laser of the appropriate wavelength and intensity so as to induce this very depolymerization reaction (retro-[4+4]-cycloaddition), these objects could be cut into predetermined shapes and into the obtained objects holes of predetermined geometry could again be cut. The new rims created by such processes would expose anthracene units, the products of the laser-induced retro-cycloaddition reaction. With the chemistry presented here, these rims could then be decorated at will employing the tools of organic chemistry. We thus foresee fascinating opportunities in the combination of 2D polymers with their defined and addressable molecular structure and synthetic chemistry. For the fluorescence label decorated sheets presented here, we further foresee the intriguing opportunities to investigate the undulation behavior of a 2D polymer in solution by time-resolved (single-molecule) fluorescence spectroscopy/microscopy once available in single-sheet form.¹⁹ With these sheets one could also contribute to the visualization of possibly existent grain boundaries (mosaicity) in the polymer single crystals. Finally, we note that edge modifications cannot be performed easily with MOFs because of their being based on equilibrium-type chemistries.²⁰

ASSOCIATED CONTENT

Supporting Information

The Supporting Information is available free of charge on the ACS Publications website at DOI: 10.1021/jacs.6b05456.

Synthesis; structure models of crystal faces (100) and (001); model studies on crystal stability; attempts to prove chemical reaction on polymer single crystal; overview CLSM images of covalently dye-labeled polymer single crystal; CLMS images of micromechanically exfoliated chemically modified 2D polymer sheet packages (PDF)

AUTHOR INFORMATION

Corresponding Author

*ads@mat.ethz.ch

Notes

The authors declare no competing financial interest.

ACKNOWLEDGMENTS

We thank the ETH Zürich for financial support. ScopeM kindly provided access to the CSLM. We thank Dr. René Verel for his competent help with solid-state NMR spectroscopy, Prof. Paul Smith and Jan Vermant for access to their optical microscopes, and Dr. Zhiqiang Ma for help with TGA-MS. We thank Daniel Messmer and Stan van de Poll for critically reading the manuscript.

REFERENCES

- (1) (a) Sakamoto, J.; van Heijst, J.; Lukin, O.; Schlüter, A. D. *Angew. Chem., Int. Ed.* **2009**, *48*, 1030–1069. (b) Payamyar, P.; King, B. T.; Öttinger, H. C.; Schlüter, A. D. *Chem. Commun.* **2016**, *52*, 18–34.

- (2) (a) Colson, J. W.; Dichtel, W. R. *Nat. Chem.* **2013**, *5*, 453–465. (b) Cai, S.-L.; Zhang, W.-G.; Zuckermann, R. N.; Li, Z.-T.; Zhao, X.; Liu, Y. *Adv. Mater.* **2015**, *27*, 5762–5770. (c) Zhuang, X.; Mai, Y.; Wu, D.; Zhang, F.; Feng, X. *Adv. Mater.* **2015**, *27*, 403–427. (d) Zang, Y.; Aoki, T.; Teraguchi, M.; Kaneko, T.; Ma, L.; Jia, H. *Polym. Rev.* **2015**, *55*, 57–89. (e) Baek, K.; Hwang, I.; Roy, I.; Shetty, D.; Kim, K. *Acc. Chem. Res.* **2015**, *48*, 2221–2229. (f) Xiang, Z.; Cao, D.; Dai, L. *Polym. Chem.* **2015**, *6*, 1896–1911. (g) Rodriguez-San-Miguel, D.; Amo-Ochoa, P.; Zamora, F. *Chem. Commun.* **2016**, *52*, 4113–4127. (h) Sakamoto, J.; Shinkai, S. *Kobunshi Ronbunshu* **2016**, *73*, 42–54.
- (3) (a) Kissel, P.; Erni, R.; Schweizer, W. B.; Rossell, M. D.; King, B. T.; Bauer, T.; Götzinger, S.; Schlüter, A. D.; Sakamoto, J. *Nat. Chem.* **2012**, *4*, 287. (b) Bhola, R.; Payamyar, P.; Murray, D. J.; Kumar, B.; Teator, A. J.; Schmidt, M. U.; Hammer, S. M.; Saha, A.; Sakamoto, J.; Schlüter, A. D.; King, B. T. *J. Am. Chem. Soc.* **2013**, *135*, 14134. (c) Kissel, P.; Murray, D. J.; Wulfstange, W. J.; Catalano, V. J.; King, B. T. *Nat. Chem.* **2014**, *6*, 774. (d) Kory, M. J.; Wörle, M.; Weber, T.; Payamyar, P.; van de Poll, S. W.; Dshemuchadse, J.; Trapp, N.; Schlüter, A. D. *Nat. Chem.* **2014**, *6*, 779.
- (4) (a) Wegner, G. *Z. Naturforsch.* **1969**, 824–832. (b) Schmidt, G. M. J. *Pure Appl. Chem.* **1971**, *27*, 647–678.
- (5) Kory, M. J.; Bergeler, M.; Reiher, M.; Schlüter, A. D. *Chem. - Eur. J.* **2014**, *20*, 6934–6938.
- (6) (a) Wu, H.; Zheng, B.; Zheng, X.; Wang, J.; Yuan, W.; Jiang, Z. *J. Power Sources* **2007**, *173*, 842–852. (b) Arora, M.; Eddy, N. K.; Mumford, K. A.; Baba, Y.; Perera, J. M.; Stevens, G. W. *Cold Reg. Sci. Technol.* **2010**, *62*, 92–97.
- (7) (a) Tanabe, K. K.; Wang, Z.; Cohen, S. M. *J. Am. Chem. Soc.* **2008**, *130*, 8508–8517. (b) Goto, Y.; Sato, H.; Shinkai, S.; Sada, K. *J. Am. Chem. Soc.* **2008**, *130*, 14354–14355. (c) Gadzikwa, T.; Farha, O. K.; Malliakas, C. D.; Kanatzidis, M. G.; Hupp, J. T.; Nguyen, S. T. *J. Am. Chem. Soc.* **2009**, *131*, 13613–13615. (d) Jung, S.; Kim, Y.; Kim, S.-J.; Kwon, T.-H.; Huh, S.; Park, S. *Chem. Commun.* **2011**, *47*, 2904–2906. (e) Ma, M.; Gross, A.; Zacher, D.; Pinto, A.; Noei, H.; Wang, Y.; Fischer, R. A.; Metzler-Nolte, N. *CrystEngComm* **2011**, *13*, 2828–2832. (f) Nagata, S.; Sato, H.; Sugikawa, K.; Kokado, K.; Sada, K. *CrystEngComm* **2012**, *14*, 4137–4141. (g) Roy, P.; Schaate, A.; Behrens, P.; Godt, A. *Chem. - Eur. J.* **2012**, *18*, 6979–6985. (h) Morris, W.; Briley, W. E.; Auyeung, E.; Cabezas, M. D.; Mirkin, C. A. *J. Am. Chem. Soc.* **2014**, *136*, 7261–7264.
- (8) (a) Yaghi, O. M.; O’Keeffe, M.; Ockwig, N. W.; Chae, H. K.; Eddaoudi, M.; Kim, J. *Nature* **2003**, *423*, 705–714. (b) Ockwig, N. W.; Delgado-Friedrichs, O.; O’Keeffe, M.; Yaghi, O. M. *Acc. Chem. Res.* **2005**, *38*, 176–182. (c) Kondo, M.; Furukawa, S.; Hirai, K.; Kitagawa, S. *Angew. Chem., Int. Ed.* **2010**, *49*, 5327–5330. (d) Zhou, H.-C.; Long, J. R.; Yaghi, O. M. *Chem. Rev.* **2012**, *112*, 673–674.
- (9) Keller, A. *Rep. Prog. Phys.* **1968**, *31*, 623.
- (10) (a) Peterlin, A.; Meinel, G. *J. Polym. Sci., Part B: Polym. Lett.* **1965**, *3*, 1059–1064. (b) Blundell, D. J.; Keller, A.; Connor, T. M. *J. Polym. Sci., Part B: Polym. Phys.* **1967**, *5*, 991–1012. (c) Fischer, E. W.; Sterzel, H. J.; Wegner, G. *Kolloid Z. Z. Polym.* **1973**, *251*, 980–990.
- (11) (a) Moon, R. J.; Martini, A.; Nairn, J.; Simonsen, J.; Youngblood, J. *Chem. Soc. Rev.* **2011**, *40*, 3941–3994. (b) Eyley, S.; Thielemans, W. *Nanoscale* **2014**, *6*, 7764–7779.
- (12) (a) Dong, S.; Roman, M. *J. Am. Chem. Soc.* **2007**, *129*, 13810–13811. (b) Nielsen, L. J.; Eyley, S.; Thielemans, W.; Aylott, J. W. *Chem. Commun.* **2010**, *46*, 8929–8931.
- (13) Qualizza, B. A.; Prasad, S.; Chiarelli, M. P.; Ciszek, J. W. *Chem. Commun.* **2013**, *49*, 4495–4497.
- (14) Calik, M.; Sick, T.; Dogru, M.; Döblinger, M.; Datz, S.; Budde, H.; Hartschuh, A.; Auras, F.; Bein, T. *J. Am. Chem. Soc.* **2016**, *138*, 1234–1239.
- (15) Baek, K.; Yun, G.; Kim, Y.; Kim, D.; Hota, R.; Hwang, I.; Xu, D.; Ko, Y. H.; Gu, G. H.; Suh, J. H.; Park, C. G.; Sung, B. J.; Kim, K. *J. Am. Chem. Soc.* **2013**, *135*, 6523–6528.
- (16) Tan, Y.-Z.; Yang, B.; Parvez, K.; Narita, A.; Osella, S.; Beljonne, D.; Feng, X.; Müllen, K. *Nat. Commun.* **2013**, *4*, 2646.
- (17) Phutdhawong, W.; Buddhasukh, D.; Pyne, S. G.; Rujiwatra, A.; Pakawatchai, C. *Synth. Commun.* **2006**, *36*, 881–883.
- (18) Qualizza, B. A.; Ciszek, J. W. *J. Phys. Org. Chem.* **2015**, *28*, 629–634.
- (19) Woll, D.; Braeken, E.; Deres, A.; De Schryver, F. C.; Uji-i, H.; Hofkens, J. *Chem. Soc. Rev.* **2009**, *38*, 313–328.
- (20) (a) Furukawa, H.; Cordova, K. E.; O’Keeffe, M.; Yaghi, O. M. *Science* **2013**, *341*, 1230444. (b) Zhou, H.-C.; Kitagawa, S. *Chem. Soc. Rev.* **2014**, *43*, 5415–5418.